Kinetics of Phosphoramide Mustard Hydrolysis in Aqueous Solution

ERIC WATSON*§, PHOEBE DEA‡, AND KENNETH K. CHAN*x

Received April 29, 1985, from the *School of Pharmacy and University of Southern California Comprehensive Cancer Center, University of Southern California, Los Angeles, CA 90033 and the ‡Department of Chemistry and Biochemistry, California State University at Los Angeles, Los Angeles, CA 90032. Accepted for publication August 16, 1985. Present address: §Amgen, 1900 Oak Terrace Lane, Thousand Oaks, CA 91320.

Abstract □ Hydrolysis of phosphoramide mustard was investigated using HPLC, ^{31}P NMR, and GC–MS with specific deuterium labels. The hydrolysis of phosphoramide mustard in sodium phosphate buffers was found to follow apparent first-order kinetics. The rate of hydrolysis was temperature and pH dependent, being slower under acidic conditions. The hydrolysis was not catalyzed by hydroxyl ion, and its pH dependence appeared to be the result of a change in the mechanism of hydrolysis at different pH values. At a pH value approximately above the pK_a of the phosphoramide mustard nitrogen, the major hydrolytic pathway of phosphoramide mustard was via the formation of the aziridinium ion, followed by nucleophilic attack. At pH values below its pK_a, cleavage of the P-N bond predominated. At pH 7.4, the formation of an aziridinium ion was followed by a rapid hydrolysis to yield the monohydroxy and, subsequently, the dihyroxy products. The hydrolysis at this pH was adequately described by consecutive first-order kinetics. Seven species in the hydrolytic mixture have been identified as intact phosphoramide mustard, *N*-(2-chloroethyl)-*N*-(2-hydroxyethyl)phosphorodiamidic acid, *N,N*-bis-(2-hydroxyethyl)phosphorodiamidic acid, phosphoramidic acid, phosphoric acid, *N,N*-bis-(2-chlorethyl)amine, and *N*-(2-chloroethyl)-*N*-(2-hydroxyethyl)amine by GC–MS with the aid of deuterium labels. Phosphoramide mustard was found to be stabilized by chloride ion. The stabilization was linearly related to the chloride ion concentration, and the mechanism was found to be via the formation of phosphoramide mustard from the aziridinium and chloride ions. Phosphoramide mustard was significantly more stable in human plasma and in 5% human serum albumin as compared to aqueous buffers, an observation that may be important in vivo.

Phosphoramide mustard, *N,N*-bis-(2-chloroethyl)phosphorodiamidic acid, (**1**), was first synthesized by Friedman and Seligman in 1954 as a potential agent for the tumor-specific release of nor-nitrogen mustard,[1] *N,N*-bis-(2-chloroethyl)amine. Subsequent preclinical[2,3] and clinical[4,5] evaluations have established **1** as a potent alkylating agent. However, this agent has also been known to be unstable, and its instability might relate to its alkylating activity. The lack of stability and pharmacokinetic information has precluded its effective use as a useful antitumor agent in clinical situations. Over the last decade, **1** has been found to be the key alkylating metabolite of cyclophosphamide (**10**), one of the most widely used alkylating agents efficacious in the treatment of a variety of neoplastic diseases. In essence, **10** is hydroxylated to form the 4-hydroxy metabolite of cyclophosphamide, **11**, by the microsomal enzymes in the liver. Compound **11** is in equilibrium with its ring open tautomer, the aldophosphamide **12**,[6-9] and these activated metabolites undergo spontaneous β-elimination to form phosphoramide mustard and acrolein. The equilibrium mixture of **11/12** is also metabolized to the 4-keto metabolite of cyclophosphamide and carboxyphosphamide. Among these metabolites, **1** is considered to be the ultimate metabolite responsible for most of the alkylating activity of **10**.[10,11]

This metabolic information has prompted several laboratories[6,2-4] to examine the stability and alkylation chemistry of **1**. This report describes the kinetics of **1** hydrolysis in detail using HPLC, GC–MS (electron impact and chemical ionization), deuterium isotope labeling, and ^{31}P NMR techniques.

Experimental Section

Materials—Phosphoramide mustard as its cyclohexylamine salt (cyclohexylammonium hydrogen-*N,N*-bis-(2-chloroethyl)phosphorodiamidate, NSC-69945) was supplied by the Drug Synthesis and Chemistry Branch, Division of Cancer Treatment, National Cancer Institute, Bethesda, MD. The purity of this material was found to be 99.0% by GC–MS, and the major impurity (ca. 1%) was characterized to be nor-nitrogen mustard. [β-$^2H_4$]phosphoramide mustard (cyclohexylammonium hydrogen-*N,N*-bis-(2,2-dideuterio-2-chloroethyl)-phosphorodiamidate, [$^2H_4$]**1**, 99.0 atom %) was synthesized by a slightly modified procedure of Colvin et al.[10] The chemical and isotopic purity of this material was found to be better than 99% by GC–MS. All chemicals and reagents: methyl iodide (MCB, Norwood, OH), Tris and 2-(bis(2-hydroxyethyl)amino)2-hydroxymethyl)-1,3-propanediol (bis-Tris) (Sigma Chemical Co., St. Louis, MO), *N,O*-bis(trimethylsilyl)trifluoroacetamide and *N*-methyl-*N*-(trimethylsilyl)trifluoroacetamide (Regis Chemical Co., Morton Grove, IL) were of analytical or reagent grade and used without further purification. Acetonitrile and methanol (J. T. Baker, Hayward, CA) were of liquid chromatographic grade. Sodium phosphate buffers[15] (pH 2.1–12.0, 0.067 M), were prepared by dilution of a 1.0 M stock solution of phosphoric acid (Sigma) with subsequent addition of sodium hydroxide (MCB) to obtain the desired pH. For pH 1.7, the concentration of the phosphoric acid was increased to 0.134 M, and a further decrease in pH to 1 required the use of 0.1 M HCl (MCB). Silver oxide was prepared from silver nitrate (MCB) by a standard procedure. C-18 reversed-phase resin was obtained from a commercial source (Analytichem International, Harbor City, CA) and packed into mini-polypropylene columns (Bio-Rad Laboratories, Richmond, CA) for extraction purposes.

Instrumentation—All HPLC determinations were carried out with a double-reciprocating pump (model 3500, Spectra-Physics, Santa Clara, CA) equipped with a variable-wavelength spectrophotometer (model 100-10, Hitachi Instruments, Santa Clara, CA) set at 207 nm to monitor intact **1**. The high-performance liquid chromatograph was operated isocratically at appropriate flow rates with either a C-18 or a C-8 reversed-phase 250 × 4.6 mm stainless steel column (Alltech Associates, Deerfield, IL).

GC analysis were carried out on a gas chromatograph (model 5710A, Hewlett-Packard, Palo Alto, CA) equipped with a nitrogen-phosphorus detector. The typical instrumental conditions used were: helium flow, 30 mL/min; hydrogen and air flows to the detector, 3 and 60 mL/min, respectively; detector voltage setting, 16.3 *V*; injector and detector temperatures, 210°C for both. All MS measurements were performed on a quadrupole mass spectrometer (model 5985 A, Hewlett-Packard, Palo Alto, CA) coupled to a gas chromatograph via an all-glass jet separator. The mass spectrometer was operated with the following parameters: transfer lines, ion source, and jet separator, all 200°C; ionization current, 300 μA; electron impact mode, electron energy at 70 eV; chemical ionization mode, electron energy at 200 eV. Isobutane (99.96% research grade, Matheson, Cucamonga, CA) was used as the chemical ionization reagent gas and was introduced directly into the source by means of an

0022-3549/85/1200-1283$01.00/0

isolation valve situated after the jet separator. For GC–MS analysis, the excess reagent was vented into the atmosphere for 1 min to minimize contamination of the ion source of the spectrometer.

The ^{31}P NMR spectra were recorded on a high-field NMR spectrometer (WM-500, USA Bruker Instruments, Inc., Manning Park, MA) operating at a field strength of 11.74 tesla (202.5 MHz ^{31}P frequency) at the Southern California Regional NMR Facility at the California Institute of Technology. Preliminary and comparative experiments were performed at the California State University at Los Angeles on a 60-MHz spectrometer (WP-60, USA Bruker Instruments) operating at 24.2 MHz for ^{31}P NMR.

Nuclear Magnetic Resonance Measurements—Sample tubes of 5 and 10 mm o.d. were used for the 60- and the 500-MHz spectrometers, respectively. All spectra were measured at 37°C. A small sealed capillary tube containing 85% phosphoric acid was placed at the center of the NMR sample tube to serve as reference for chemical shift as well as an internal standard for spectral intensity calibrations.

In the degradation kinetics measurements, an NMR sample tube containing 1 M Tris (sulfate) buffer (pH 7.4) in a 1:1 mixture of ^2H_2O:H_2O was equilibrated at a probe temperature of 37°C. The tuning for probe and field homogeneity was carried out on the sample. An appropriate volume of this buffer solution was then added to a preweighed sample of **1** such that the initial concentration was 0.5 M. Proton-decoupled spectra were recorded with a 40-ppm sweep width and an r.f. pulse of 20 μs. The time interval between each time-averaged spectrum was 1.28 min.

Hydrolysis of Phosphoramide Mustard at Different pH Values and Temperatures—Solutions of **1** at 8 mM each in 0.067 M sodium phosphate buffer were incubated separately at temperatures of 0°C, 25°C, and 37°C. At each temperature, hydrolysis studies were carried out at different pH values[15] from 1.0 to 12.0. Aliquots of the solution of **1** were removed at various time intervals, and 20-μL aliquots were injected directly into the HPLC equipped with a 10-μm C-18 reversed-phase column. The system was eluted with acetonitrile: 0.005 M perchloric acid, 20:80, at a flow rate of 1.6 mL/min. Theophylline was used as the internal standard in some experiments, such as those at 0°C, where the rate of hydrolysis was slow. Under these conditions, the retention times for **1** and theophylline were 5.0 and 7.0 min, respectively.

At low pH values, between 1.7 and 2.1, solutions of **1** at 8 mM were each prepared in appropriate concentrations of phosphoric acid, and at pH 1.0, **1** in 0.1 M HCl was used. These solutions were incubated at 38°C, and split aliquots were removed at various time intervals. One set of the aliquots was analyzed for **1** and degradation products by HPLC as described above. The duplicate sets were analyzed for nor-nitrogen mustard (**6**) by a GC assay in which a 1-μL aliquot of the hydrolysate was injected directly onto the GC equipped with a 183 × 2 mm i.d. 3% Poly A 103 column maintained at 140°C. Under these conditions, nor-nitrogen mustard was eluted with a retention time of 1.0 min.

Analysis of Degradation Intermediates and Products from Phosphoramide Mustard—A solution of **1** at 8 mM was incubated in 0.067 M, pH 7.4 sodium phosphate buffer at 37°C. At suitable time intervals, 0.1-mL aliquots of the hydrolysate were removed and immediately analyzed by HPLC, with a 10-μm C-8 reversed-phase column and 0.005 M perchloric acid at a flow rate of 1.0 mL/min as the eluting solvent. Theophylline was used as the internal standard. Under these conditions, one hydrolysis intermediate [subsequently identified as *N*-(2-chloroethyl)-*N*-(2-hydroxyethyl)phosphodiamidic acid, **3**], **1**, and the internal standard gave retention times of 4.0, 6.0, and 7.5 min, respectively. In another set of experiments, in which all conditions were kept constant except that the eluant was replaced with distilled water, a more polar component [subsequently identified as *N*,*N*-bis-(2-hydroxyethyl)phosphodiamidic acid, **5**, by GC–MS] appeared with time and gave a retention time close to the solvent front.

Stability of Phosphoramide Mustard at Various Concentrations of Chloride Ion and the Interaction with KBr—To five 8 mM solutions of **1** in 0.067 M, pH 7.4 sodium phosphate buffer were added various amounts of NaCl such that the resulting chloride ion concentrations were 0.14, 0.5, 1.0, 1.5, and 2.0 M, respectively. A similar solution of **1** containing 1.0 M KBr was also prepared to study the interaction of **1** with bromide ion. These solutions were incubated at 37°C. At different time intervals, aliquots of the solutions were removed for **1** analysis by HPLC. In the presence of bromide ion, a new component was eluted in the HPLC approximately 1 min after **1**. The HPLC effluent corresponding to the emergence of this component was repeatedly collected. After lyophilization, the residue was kept at −20°C until analysis by GC–MS.

Isolation of *N*-(2-Chloroethyl)-N-(2-hydroxyethyl)phosphodiamidic Acid—A solution of **1** at 8 mM in 0.067 M, pH 7.4 sodium phosphate buffer was incubated at 38°C for 30 min. Aliquots of the solution were repetitively injected onto the HPLC and eluted with pH 2.8 dilute trifluoroacetic acid. The use of perchloric acid was not feasible because of the interference in the derivatization step for GC–MS identification. The fractions corresponding to **1** and **3** were collected separately into several 50-mL, round-bottomed flasks which were kept in a dry ice–acetone bath. These fractions were then lyophilized, and the residues were kept at −20°C for various experiments described below.

Hydrolysis of *N*-(2-Chloroethyl)-*N*-(2-hydroxyethyl)phosphodiamidic Acid and Effect of NaCl—Isolated **3** was dissolved in an appropriate volume of pH 7.4, 0.067 M sodium phosphate buffer such that a 20-μL aliquot of the resultant solution gave rise to an HPLC response comparable to that of **3** when generated from hydrolysis of an 8 mM of solution of **1** at 30 min under the conditions described previously. The solution was incubated at 37°C, and aliquots were removed at different times for HPLC analysis for remaining **3**. To a separately prepared solution of **3** was added an appropriate amount of NaCl to result in a 2.0 M chloride ion concentration. The resultant solution was then incubated at 38°C. Aliquots were removed at different times for HPLC analyses.

Stability of Phosphoramide Mustard in Tris Chloride and Tris Sulfate—Solutions of **1**, 50 mM each in 1.0 M of Tris chloride and Tris sulfate, were incubated separately at 38°C. Aliquots were removed at different times for **1** analysis by the same HPLC procedure as previously described for hydrolysis of **1**. Theobromine was used as the internal standard as Tris buffer interfered with theophylline under these conditions.

Mass Spectrometric Analysis—For structural identification, solutions of **1** at 8 mM in either pH 7.4, 0.067 M sodium phosphate buffer or distilled water (for analysis of phosphate) were allowed to degrade at 37°C for 40, 60, and 180 min. The hydrolysates were then lyophilized, and the residues were kept at −20°C until analysis. Similarly, [$^2H_4$]**1** solutions were hydrolyzed and processed in the same fashion. Specific components from the hydrolytic or incubation mixture as previously described were isolated from HPLC and lyophilized. The residues were also kept at −20°C until use. These lyophilized products or residues were then treated with a mixture of *N*,*O*-bis-(trimethylsilyl)trifluoroacetamide–pyridine, 4:1, at room temperature for a period of 1 to 10 min. Aliquots of 1 μL each were injected into the GC–MS and the identification of the trimethylsilyl derivatives of **1** and its hydrolytic products was accomplished in the chemical ionization mode. A glass column (1.8 m × 2 mm i.d.) packed with 1% OV-101, 100/120 mesh Gas Chrom Q was used. The oven temperature was programmed from 150°C to 240°C at 18°C/min. In some cases, a 3% OV-1 column was used at a lower programmed temperature from 100 to 260°C. Helium was used as the carrier gas at a flow rate of 25 mL/min throughout these experiments. For the structural identification of monobromo **1**, the residue obtained from incubation of solution of **1** with KBr as described previously was also silylated with *N*,*O*-bis-(trimethylsilyl)trifluoroacetamide–pyridine. A 1-μL aliquot was analyzed by direct-probe MS with isobutane chemical ionization.

For kinetic studies of **1** involving chloride ion, solutions of [$^2H_4$]**1** were prepared (8 mM in 0.067 M, pH 7.4, sodium phosphate buffer) which contained various amounts of sodium chloride to achieve chloride ion concentrations of 0, 0.5, 1.0, and 2.0 M, respectively. These solutions were kept at 38°C, with aliquots removed at 0, 5, 10, 15, 20, 25, 30, 34, 40, 50, 60, 70, 80, and 100 min. These aliquots were lyophilized, and the residues were methylated according to the procedure of Bryant et al.[16] Essentially, the residue was refluxed for 15 min with approximately 100 mg of silver oxide, 50 mg of anhydrous potassium carbonate, and a 1:1 (v/v) mixture (1.5 mL) of methyl iodide and acetonitrile. The organic phase was evaporated, and the residue was dissolved in 1 mL of ethyl acetate, which was then reduced in volume to approximately 250 μL under a stream of N_2. A 1-μL aliquot was injected into the GC–MS operating in the electron impact mode. The GC conditions were similar to those described above for structural identification, except in this case, the column temperature was isothermally maintained at 220°C. Under these conditions, trimethyl **1** was eluted in 4 min. For quantitation of unlabeled and labeled **1** and the extent of scrambling, ions at *m/z*

213, 215, 217, and 219 were monitored using the selected ion monitor mode (SIM).

For quantitation of 1 in human plasma or 5% human serum albumin solution, 10 μg of [$^2H_4$]1 was added to 0.1 mL of the sample containing 1, and the final volume was adjusted to 0.5 mL with distilled water. Approximately 1 mg of nitrogen mustard and 3 drops of 2 M HCl were added, and the entire sample was transferred to 0.4 g of C-18 reversed-phase resin in a 10-mL polypropylene column. The column was centrifuged at 1000 rpm for 3 min, washed with 0.5 mL of cold water, and centrifuged again at 1000 rpm for 3 min. Compound 1 was eluted from the column with the addition of 1 mL of cold methanol, followed by centrifugation at 1000 rpm for 2 min. The methanol was evaporated under N_2 in culture tubes placed on the surface of a 50°C sand bath. The residue was dissolved in 50 μL of *N*-methyl-*N*-(trimethylsilyl)trifluoroacetamide and the solution was heated for 20 min at 120°C. A 2-μL aliquot of the solution was subjected to GC–MS analysis. Ions at *m/z* 329 and 333, corresponding to [M − HCl]$^+$ fragment for trimethylsilyl derivatives of 1 and [$^2H_4$]1, respectively, were monitored by SIM.

Stability of Phosphoramide Mustard in Fresh Human Plasma and 5% Human Serum Albumin. The stability of 1 in human plasma was determined by adding 550 μg of 1 to 5.5 mL of freshly collected human plasma. After a brief period of sonication and vortexing, the mixture was incubated at 37°C. Aliquots of 0.1 mL were removed at different times and analyzed for 1 concentration by GC–MS as described previously. Similar experiments were performed with 5% human serum albumin solution instead of plasma.

Results

Phosphoramide Mustard Stability in Phosphate Buffers—The proposed overall hydrolysis pathways of 1 are shown in Scheme I. Figure 1 shows the HPLC chromatogram obtained from a freshly prepared solution of 1 and the internal standard theophylline. These two peaks were well resolved, and completely degraded solutions of 1 did not contain components with the same retentions. Concentrations of 1 were obtained by calculations with either peak height or peak height ratio methods.

The hydrolyses of 1 were carried out at 0°C, 25°C, and 38°C over a pH range from 1.0 to 12.0. All hydrolysis profiles were found to exhibit linear relationships (regression coefficients greater than 0.98) when the logarithmic values of residual concentrations of 1 were plotted as a function of time. Several typical plots at 25°C and 38°C are shown in Fig. 2. Thus, hydrolysis of 1 appears to follow apparent first-order kinetics. Table I summarizes the rate constants and their corresponding half-lives, as computed by linear regression analysis, showing the effects of temperature and pH on the overall stability of 1. Data substantiated the expectant

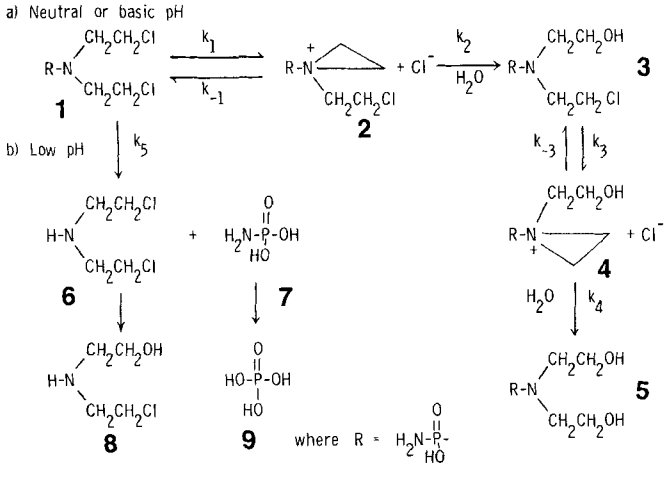

Scheme I—Hydrolytic pathways of phosphoramide mustard.

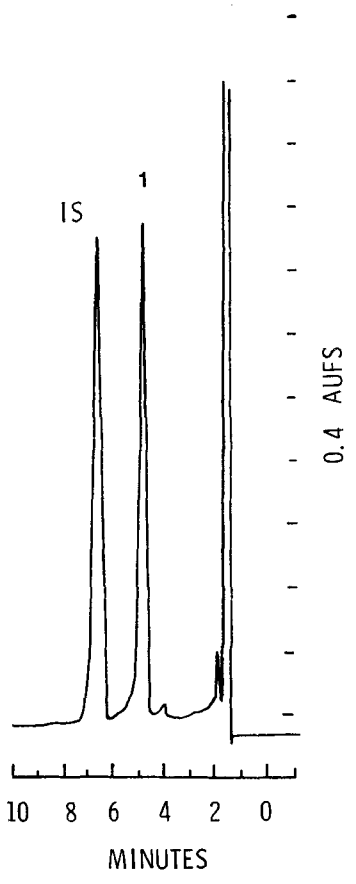

Figure 1—*HPLC chromatogram of phosphoramide mustard in phosphate buffers. IS, Internal standard theophylline.*

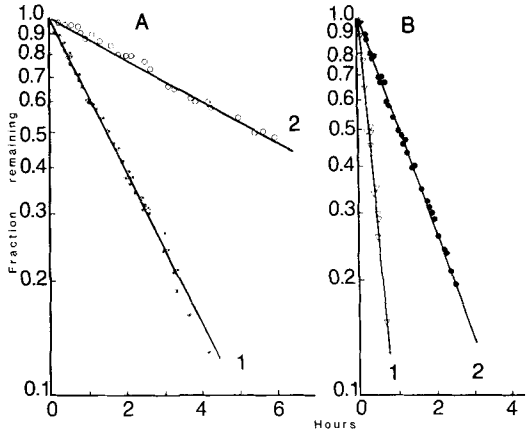

Figure 2—*Semi-log plots for fraction phosphoramide mustard remaining at (A) 25 °C, pH 7.4 (1) and pH 1.7 (2); and (B) 38 °C, pH 7.4 (1) and pH 1.7 (2).*

endothermic nature of the overall hydrolysis reaction. In addition, the pH–rate profile as observable in Table I and Fig. 3 exhibited a gradual increase in the rate from pH 1.7 to approximately 5.0, then reached a plateau region onward to pH 12.0.

The hydrolysis of 1 at low pH was investigated in detail by using HPLC and GC. In 0.1 M HCl and at 38°C, nor-nitrogen mustard was found to be the predominant hydrolysis product formed in the 250-min period measured, corresponding to approximately 85% of the initial amount of 1, and no 3 was detected by HPLC. When concentrations of both 1 and nor-

Table I—Effect of pH and Temperature on the Stability of Phosphoramide Mustard in Sodium Phosphate Buffers[a]

Temp[b]	pH	Rate Constant,[c] min^{-1}	n	$t_{1/2}$, min
0°C	1.9	0.0000539 (0.0000005)	2	12,780
	7.4	0.000103 (0.000003)	2	6,720
	12.0	0.0000960 (0.0000003)	2	7,198
25°C	1.7	0.00210 (0.00002)	2	329.5
	3.0	0.00324 (0.00003)	2	214.2
	4.0	0.00517 (0.00002)	2	134.2
	7.4	0.00744 (0.00026)	2	93.2
	10.0	0.00693 (0.00047)	2	100.4
	12.0	0.00693 (0.00011)	2	100.0
38°C	1.7	0.0111 (0.0001)	2	62.5
	2.0	0.0130 (0.0002)	2	53.2
	2.5	0.0119 (0.0003)	2	58.2
	3.0	0.0208 (0.0026)	2	33.9
	3.5	0.0310 (0.0004)	2	22.4
	4.0	0.0430 (0.0012)	2	16.1
	5.0	0.0487 (0.0003)	2	14.2
	6.0	0.0590 (0.0007)	2	11.7
	7.4	0.0486 (0.0050)	6	14.4
	9.0	0.0566 (0.0013)	3	12.2
	10.0	0.0592 (0.0006)	3	11.8
	11.0	0.0573 (0.0006)	3	12.1
	12.0	0.0528 (0.0046)	2	13.3

[a] See *Experimental Section* and reference 15 in text for preparation of buffers. [b] Values are ± 1°C. [c] Obtained from linear regression on semilogarithmic expressions. Values in parentheses are deviations or SD.

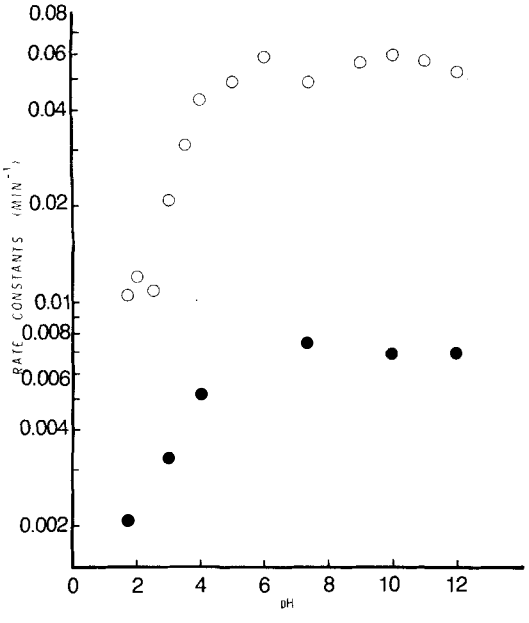

Figure 3—*Effect of pH on the rate of hydrolysis of phosphoramide mustard at 25 °C (●) and at 37 °C (○).*

nitrogen mustard were followed simultaneously in 0.067 M phosphoric acid (pH 2.1) to avoid possible stabilization by chloride ion, 1 was found to degrade according to apparent first-order kinetics, yielding a decay rate constant essentially equal to the rate constant of formation for nor-nitrogen mustard as estimated by the sigma minus plot[17] (Fig. 4).

Phosphoramide Mustard Stability in Tris Buffers—In 1.0 M Tris sulfate buffer at pH 7.4 and 38°C, 1 at 50 mM was found to undergo apparent first-order hydrolysis with a rate constant of 0.0371 ± 0.001 min^{-1} (n = 4) or a half-life ($t_{1/2}$) of

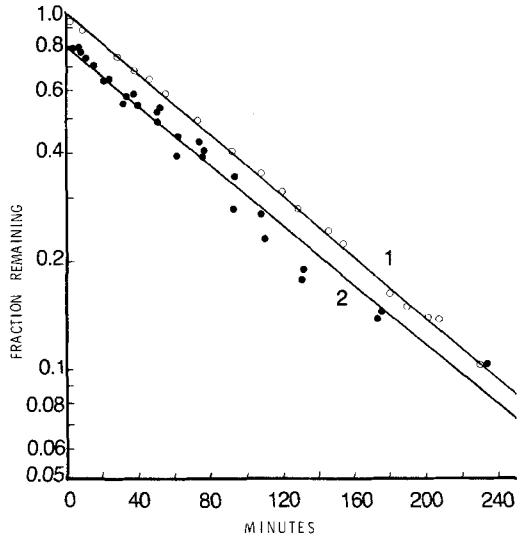

Figure 4—*Hydrolysis of phosphoramide mustard at 38 °C in 0.067 M, pH 2.1 phosphoric acid. Key: phosphoramide mustard (1); nor-nitrogen mustard (2), expressed in fraction remained to be formed.*

18.7 min. Under identical conditions, however, when Tris chloride was used, a solution of 1 was also found to undergo apparent first-order decay, but with a smaller rate constant of 0.0261 ± 0.001 min^{-1} or a $t_{1/2}$ of 26.6 min. The increase in stability of 1 in Tris chloride buffer may be due to the chloride ion stabilization effect (see discussion on chloride ion stabilization below).

Phosphorus-31 Nuclear Magnetic Resonance Studies. A stacked plot of the ^{31}P NMR spectra of 0.5 M of 1 as a function of time is shown in Fig. 5. The ^{31}P resonance for 1 appeared at 13.8 ppm downfield from phosphoric acid. This is comparable to the chemical shift value of 13.2 ppm previously reported[14] for 1, where 0.25% v/v phosphoric acid in ^2H_2O was used as external reference. The chemical shift of phosphoric acid is known to vary with pH,[19] the chemical shift moving upfield with increasing phosphoric acid concentrations. The signal intensity of the ^{31}P resonance of 1 was observed to decrease as a function of time. The disappearance of 1 followed apparent first-order kinetics (Fig. 6), yielding a $t_{1/2}$ of 16.9 ± 0.3 min (n = 2) as obtained from regression analysis. As the ^{31}P resonance for 1 decreased, several new

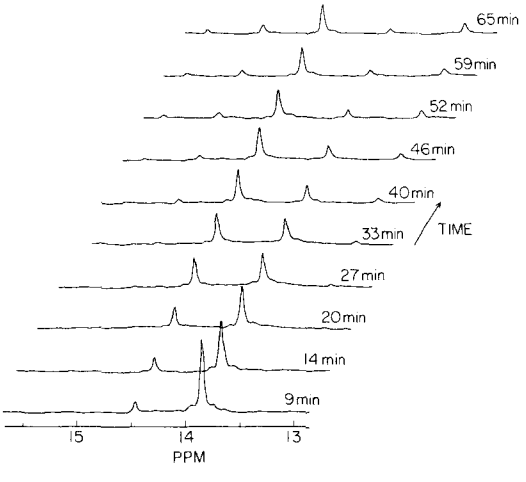

Figure 5—*Stacked plot of ^{31}P NMR spectra of phosphoramide mustard in 1.0 M, pH 7.4 Tris buffer at 37 °C.*

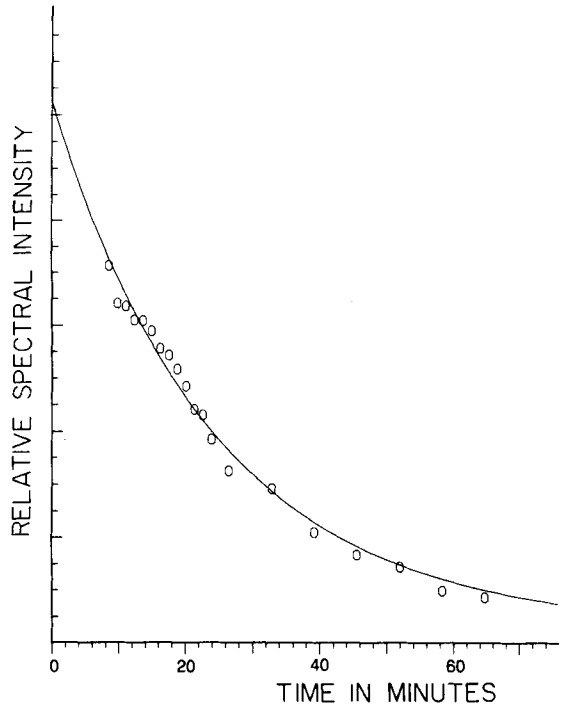

Figure 6—*Disappearance of phosphoramide mustard as measured by ^{31}P NMR. Open circles are experimental data and solid line is the computer curve fitted to a first-order decay equation.*

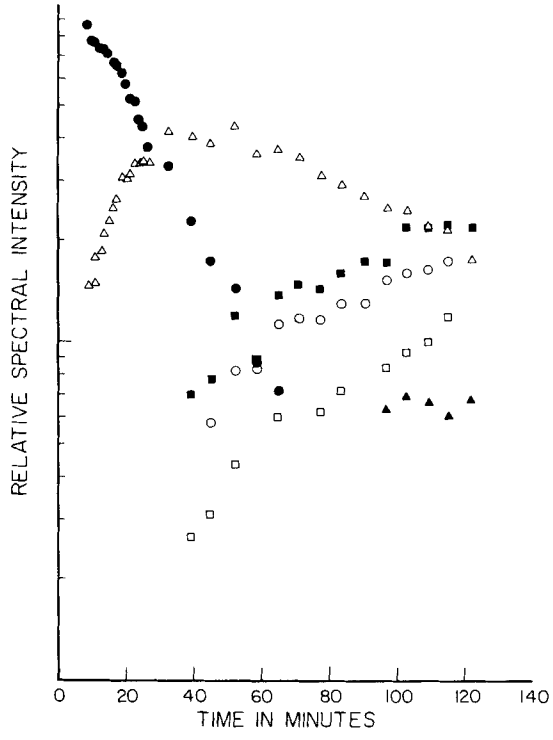

Figure 7—*Phosphorus containing species as detected in the phosphoramide mustard hydrolysate at different times by ^{31}P NMR. The chemical shifts of these species (in parts per million) are: (□) 3.34; (●) phosphoramide mustard at 13.84; (■) 13.10; (△) 14.47; (○) 15.02; (▲) 15.53.*

phosphorus signals, corresponding to intermediates or end products of the decomposition kinetics, appeared. At the end of 2 h, five signals were readily detectable, appearing in the order of decreasing signal intensity at 13.10, 15.02, 14.47, 3.34, and 15.53 ppm. Their spectral intensities relative to those of 1 as a function of time are shown in Fig. 7.

Identification of the Degradation Products of Phosphoramide Mustard—During the course of the stability studies using HPLC and ^{31}P NMR methods, degradation intermediates and/or end products were observed. With time of incubation, a more polar component (component III) first appeared, followed by an even more polar compound (component V), which eluted close to the solvent front (Fig. 8). Identification of components III and V was carried out by GC–MS. The residues obtained from 1 and [$^2H_4$]1 40-min hydrolysates were silylated and analyzed by GC–MS with an OV-101 column under conditions described previously. Figure 9 shows the total ion chromatogram of these derivatives with three major components. The molecular and quasi-molecular ions and their fragments of several of the silyl derivatives of these components are listed in Table II. On the basis of these mass spectral data, components I, III, and V were tentatively identified as 1, 3, and 5, respectively. When a 3% OV-1 column was used at a lower programmed temperature from 100 to 260°C, several other, more volatile derivatives were revealed with richer composition in the 60- and 180-min hydrolysates. On the basis of the mass spectral data for the hydrolyses of 1 and the labeled 1 (Table II), these compounds were tentatively identified as nor-nitrogen mustard 6, phosphoramidic acid 7, phosphoric acid or phosphate 9, and monohydroxy nor-nitrogen mustard, 8, 2-hydroxyethyl-2-chloroethylamine). The identities for phosphoric acid, 1, phosphoramidic acid, and nor-nitrogen mustard were further confirmed by the use of authentic samples. Their silyl derivatives gave mass spectra and retention times identical to those of the respective components under consideration. When a

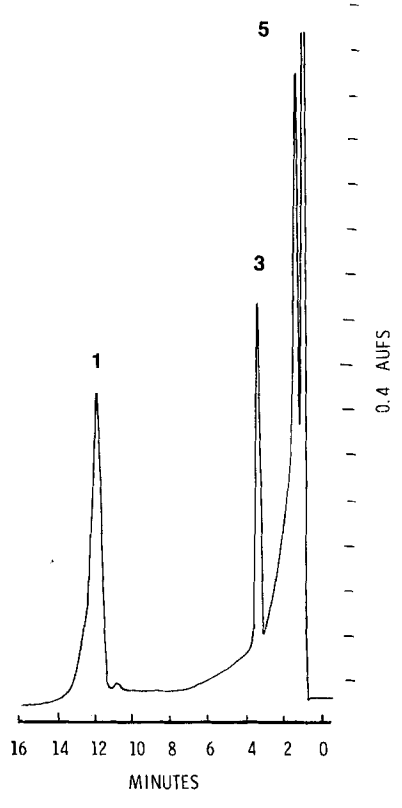

Figure 8—*High-performance liquid chromatogram of phosphoramide mustard and its hydrolytic products. 1, intact phosphoramide mustard, 1; 3, N-(2-chloroethyl)-N-(2-hydroxyethyl)phosphodiamidic acid; 5, N,N-bis(2-hydroxyethyl)phosphodiamidic acid.*

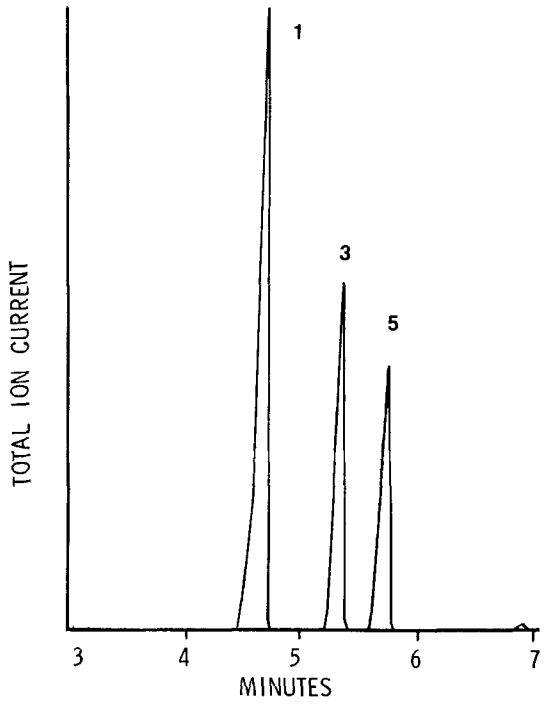

Figure 9—*GC–MS total ion chromatogram of trimethylsilyl derivatives of phosphoramide mustard and its degradation products. 1, Pertrimethylsilyl phosphoramide mustard; 3, pertrimethylsilyl N-(2-chloroethyl)-N-(2-hydroxyethyl)phosphodiamidic acid; 5, pertrimethylsilyl N,N-bis(2-hydroxyethyl)phosphodiamidic acid.*

sample of **6** was allowed to hydrolyze in distilled water for 10 min, followed by lyophilization and silylation, the residue gave rise to one major component which gave a mass spectrum and GC retention time identical to those of the component **9**. This evidence confirms the assigned structure of monohydroxy nor-nitrogen mustard. The identities of **3** and **5** were further supported by the elution behavior on the reversed-phase column under the employed HPLC conditions and their time sequence of generation during hydrolysis of **1** as monitored by HPLC. The component appearing first in time sequence (component III), when isolated and derivatized by silylation, gave a mass spectrum identical to that of **3**. Similarly, the slower-appearing component (component V) under the same treatment gave a mass spectrum identical to that of **5**. Component V had a shorter retention than component III, indicating the more polar characteristics of the former. Of the remaining degradation products, phosphate and phosphoramidic acid were found to elute with the solvent front, while nor-nitrogen mustard and its monohydroxy product could not be located on the HPLC chromatogram since these compounds lack a UV chromophore at 207 nm.

Effect and Mechanism of Chloride Ion Stabilization on Phosphoramide Mustard Solution. The effect of chloride ion stabilization on solutions of **1** was studied. Compound **1** was incubated with increasing concentrations of chloride ion at 38°C and pH 7.4. The $t_{1/2}$ were found to increase from 18 to 63 min, corresponding to the addition of 0–2.0 M chloride, respectively (Fig. 10). The mechanism of chloride ion stabilization could be conceived as due to the reverse attack by the internal chloride ion present (internal return) or the external chloride ion added to the system. This mechanism was investigated by the use of **1** labeled with deuterium in the β-position. According to Scheme I, the formation of aziridinium ion renders the two ethylene carbons symmetrical. The reverse reaction should result in scrambling of the labels (see Scheme IIA). When scrambling occurs, α-cleavage of the trimethyl derivative of [β-$^2H_4$]**1** under electron impact conditions is expected to yield mass fragments at *m/z* 217 and 219, while the lack of scrambling should give similar fragments at *m/z* 215 and 217 (see Scheme IIB). Thus, the ratio of 215/219 was used as an indicator, and the increase in this ratio with time was indicative of scrambling and reversal of the aziridinium ion formation. Figure 11 shows the ratio plots with

Table II—Mass Spectral Data[a] of Trimethylsilyl Derivatives of Phosphoramide Mustard (1) and [β-$^2H_4$]Phosphoramide Mustard and Their Hydrolytic Products.

Species[b]	*m/z*, (Relative Intensity)		Proposed Structure
	1	[β-$^2H_4$]**1**	
1	437 (100)	442 (100)	$[M + 1]^+$ (^{35}Cl)
	439 (83)	443 (81)	$[M + 1]^+$ (^{37}Cl)
	401 (3)	403 (3)	$[M + 1-Cl]^+$
	365 (22)	369 (40)	$[M + 1-(CH_3)_2Si{=}CH_2]^+$ (^{35}Cl)
	367 (14)	371 (25)	$[M + 1-(CH_3)_2Si{=}CH_2]^+$ (^{37}Cl)
	329 (18)	333 (10)	$[M + 1-(CH_3)_3SiCl]^+$ (^{35}Cl)
	331 (6)	335 (3)	$[M + 1-(CH_3)_3SiCl]^+$ (^{37}Cl)
3	491 (100)	495 (33)	$[M + 1]^+$ (^{35}Cl)
	493 (49)	497 (18)	$[M + 1]^+$ (^{37}Cl)
	419 (65)	423 (33)	$[M + 1-(CH_3)_2Si{=}CH_2]^+$ (^{35}Cl)
	421 (28)	425 (46)	$[M + 1-(CH_3)_2Si{=}CH_2]^+$ (^{37}Cl)
5	545 (100)	549 (58)	$[M + 1]^+$
	473 (81)	477 (100)	$[M + 1-(CH_3)_2Si{=}CH_2]^+$
6	214 (40)	218 (40)	$[M + 1]^+$ (^{35}Cl)
	216 (26)	220 (26)	$[M + 1]^+$ (^{37}Cl)
	178 (100)	182 (100)	$[M + 1-HCl]^+$ (^{35}Cl)
	180 (35)	184 (35)	$[M + 1-HCl]^+$ (^{37}Cl)
7[c]	314 (100)	314 (100)	$[M + 1]^+$
8[d]	196 (100)	200 (100)	$[M + 1]^+$ (^{35}Cl)
	198 (40)	202 (30)	$[M + 1]^+$ (^{37}Cl)
9	315 (100)	315 (100)	$[M + 1]^+$

[a] All derivatives were analyzed as pertrimethylsilyl derivatives except those indicated under isobutane chemical ionization. [b] See Scheme I for structures. Compound numbers: **3**, *N*-(2-chloroethyl)-*N*-(2-hydroxyethyl) phosphodiamidic acid; **5**, *N,N*-bis(2-hydroxyethyl)phosphodiamidic acid; **6**, nor-nitrogen mustard; **7**, phosphoramidic acid; **8**, monohydroxy nor-nitrogen mustard (2-hydroxyethyl-2-chloroethylamine); **9**, phosphoric acid or phosphate. [c] As tri-trimethylsilyl derivative. [d] As monotrimethylsilyl derivative.

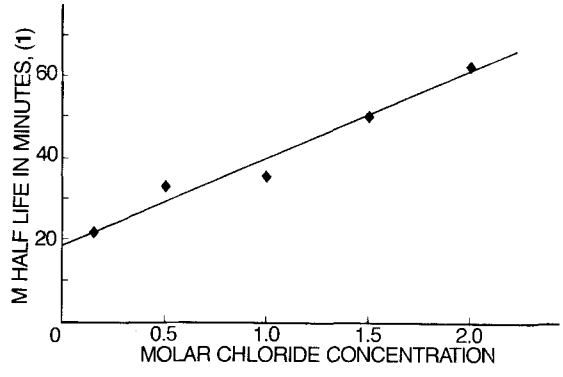

Figure 10—*Effect of chloride ion on the rate of phosphoramide mustard hydrolysis at 38 °C in sodium phosphate buffer at pH 7.4 (see text for details).*

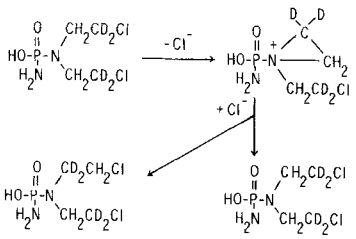

Scheme IIA

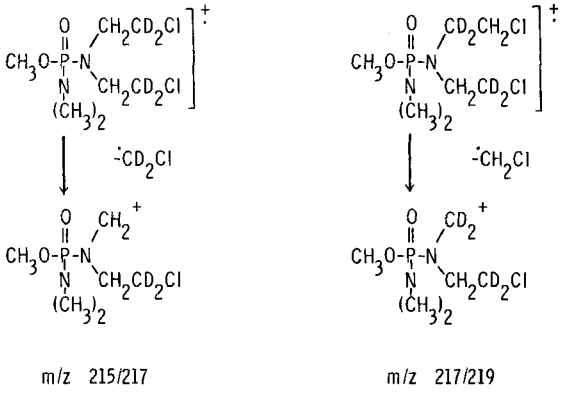

Scheme IIB

Scheme II—(A) Possible modes of chloride attack on phosphoramide mustard in solution. (B) Ions generated from α-cleavage of deuterated trimethyl phosphoramide mustard under electron impact conditions.

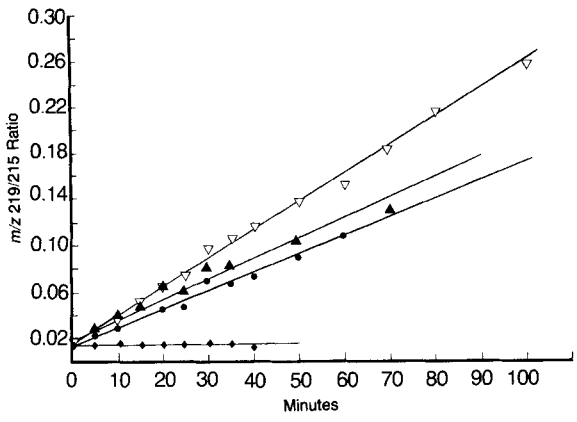

Figure 11—*Effect of chloride ion concentration on ion ratio at* m/z *219:215 after incubation with [β-$^2H_4$]phosphoramide mustard. Key:* (◆) *no sodium chloride added;* (●) *0.5 M chloride ion;* (▲) *1.0 M chloride ion;* (△) *2.0 M chloride ion.*

time of solutions of 1 at 0, 0.5, 1.0, and 2.0 M chloride concentrations. As shown, in the absence of the addition of sodium chloride, *m/z* 215/219 ratio was very low and remained constant up to a period of 100 min monitored, indicating no appreciable internal return or reversal of the cyclization process during this period. With sodium chloride addition, however, the ratio increased with time, and the rate of increase was essentially parallel to the increase in chloride concentration. To obtain further evidence for the attack of the aziridinium ion by an external nucleophile, 1 was incubated with 1.0 M KBr at 38°C for 30 min to form the monobromo derivative, which gave ions at *m/s* 481 and 483, corresponding to $[M + 1]^+$ and its bromine isotope ion, respectively.

Stability of Phosphoramide Mustard in Plasma—The profiles of 1 degradation in fresh human plasma as well as 5% human serum albumin are shown in Fig. 12. The concentrations of 1 in cases were found to decline with apparent first-order rate processes, yielding a half-life of 64.2 and 68.5 min (n = 2), respectively, in plasma and in 5% human serum albumin.

Discussion

Chloride ion release,[20,22] colorimetric reaction,[23] and thiosulfate titration[24,25] have been the classical analytical methods for studying degradation kinetics of nitrogen mustard-containing compounds; however, these methods are indirect and lack specificity. For compounds capable of undergoing multiple hydrolytic pathways such as 1, a number of species are generated simultaneously or sequentially, and these species could react with nucleophilic agents or release chloride ion. Thus, in this report rapid HPLC was used for the quantitation of 1 and several of the intermediates. The HPLC method was augmented by ^{31}P NMR, GC, GC–MS, and specific stable isotope labeling techniques, providing data for the elucidation of the rather complex degradation of 1.

Kinetics of Phosphoramide Mustard Hydrolysis—As shown in Fig. 2 and Table I, hydrolysis of 1 in phosphate buffer appears to follow apparent first-order kinetics as measured by HPLC. The observed apparent first-order kinetics of 1 hydrolysis is also supported by the results from the ^{31}P NMR studies shown in Fig. 6. In 1 M Tris (sulfate) buffer, pH 7.4 at 37°C, the phosphorus signal of 1 was found to decline monoexponentially with a $t_{1/2}$ of 16.8 ± 0.3 min. This result is similar to 16.0 min obtained in sodium phosphate buffer and to 18.7 min in Tris sulfate at the same pH by HPLC and is nearly identical to that recently reported by Engle et al.,[14] using primarily ^{31}P NMR techniques. Therefore, the results from ^{31}P NMR and from HPLC under similar conditions were not significantly different.

The hydrolysis proceeds at a faster rate at a higher temperature but is stabilized at a lower temperature. Thus, at 0°C, the $t_{1/2}$ of the solution of 1 becomes 115 h, more than a 10-fold increase in stability relative to that at room tempera-

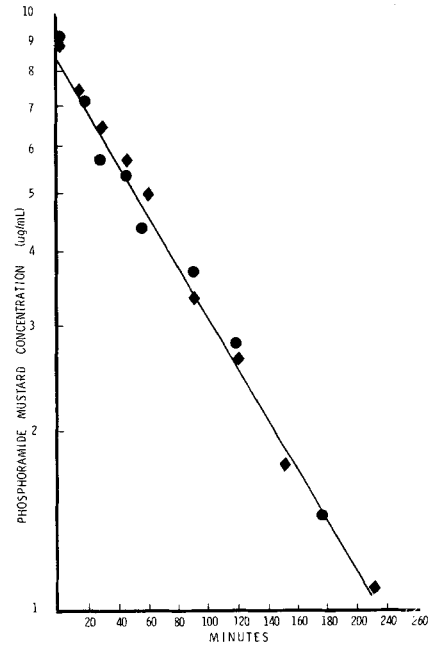

Figure 12—*Stability of phosphoramide mustard in 5% human serum albumin* (●) *and in fresh human plasma* (◆) *at 38 °C.*

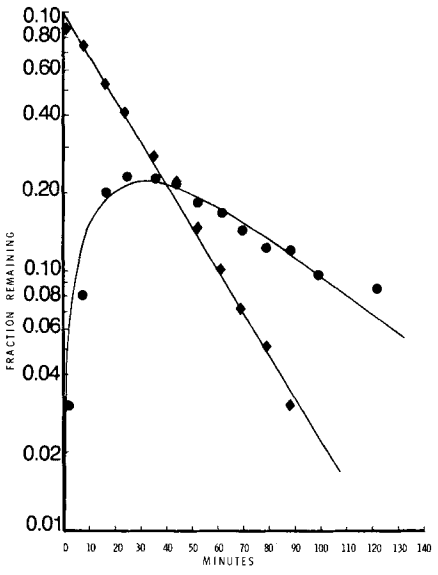

Figure 13—*Semi-log plots of hydrolysis profiles of phosphoramide mustard (◆) and N-(2-chloroethyl)-N-(2-hydroxyethyl)phosphodiamidic acid (●) in pH 7.4, 0.067 M sodium phosphate buffer at 38 °C. Solid lines were obtained from computer regressions to eqs. 1 and 2.*

ture. The rate of hydrolysis of **1** appears to be pH dependent, decreasing rapidly with a decrease in pH. As shown in Table I and Fig. 3, at pH above 5, the hydrolysis profile shows a plateau region, which indicates that **1** degradation is not catalyzed by hydroxide ion. At pH below 5, the stability of **1** increases with a decrease in pH. The stabilization may be attributable to the protonation of the nitrogen atom in the nitrogen mustard side chain (pathway b, Scheme I), thereby retarding the ability of aziridinium ion formation. This protonation may facilitate the cleavage of the P-N bond such that at pH 2.1 nor-nitrogen mustard became the major degradation intermediate of **1** and no appreciable formation of **3** was evident. The kinetics of **1** hydrolysis at this pH was also found to be apparent first-order, with a rate constant approximately equal to that of nor-nitrogen mustard formation, consistent with the proposed pathway (Fig. 4). Thus, cleavage of the P-N bond appears to be the major hydrolytic pathway of **1** under acidic conditions, whereas under neutral and basic conditions, **1** undergoes hydrolysis through the formation of aziridinium ion.

The kinetics of **1** hydrolysis at pH 7.4 were studied in detail. Concentrations of both **1** and **3** were measured over time, and a typical profile as expressed in **1** equivalents is shown in Fig. 13. As shown in this figure, **3** was generated from **1**, and the concentration increased with time. After reaching a peak level at 30 min, the concentration of this species decreased in an apparent first-order manner, with a $t_{1/2}$ of approximately 25 min. Due to the large overlap of the peak of **5** with the solvent front, its accurate measurement was more difficult. In one experiment, the levels of this component were found to accumulate while concentrations of **3** decreased. The levels of **5** also declined monoexponentially after reaching a peak (result not shown). The kinetics of **1** hydrolysis can be approximated by consecutive first-order kinetics as shown below, on the basis of the pathway a in Scheme I, assuming that $k_1,k_{-1} >> k_2$ and $k_3,k_{-3} >> k_4$:

$$\mathbf{1} \xrightarrow{k_2} \mathbf{3} \xrightarrow{k_4} \mathbf{5}$$

where the rate processes are depicted by the following equations:

$$\mathbf{1} = \mathbf{1}_o\exp(-k_2t) \quad (1)$$

$$\mathbf{3} = \mathbf{1}_o k_2[(k_4 - k_2)][\exp(-k_2t) - \exp(-k_4t)] \quad (2)$$

By use of the computer program FIGS (courtesy of Dr. Michael Bolger, University of Southern California, Los Angeles) on an IBM personal computer, kinetic data were analyzed by nonlinear regression fitting to eqs. 1 and 2. In most cases, none of the parameters were constrained. In two sets of data, it was necessary to obtain k_2 first from fitting the data of **1** to eq. 1 and to hold it invariant in eq. 2 in order to achieve satisfactory minimization. Most of the data were weighted to the square of the reciprocal concentrations, and the usual criteria of error minimization were used for the nonlinear regression. The rate constants k_2 and k_4 thus obtained are 0.0433 ± 0.0061 (n = 6) and 0.03100 ± 0.0112 (n = 4) min^{-1}, respectively, with corresponding $t_{1/2}$ of 16.0 and 22.4 min. Another recently developed procedure, in which statistical moment theory is utilized for estimating rate constants for consecutive first-order kinetics,[26,27] was also used, yielding k_4 of 0.03219 ± 0.01206 min^{-1} or $t_{1/2}$ of 24.8 min (n = 4). Thus, these two independent methods for kinetic data analysis provide results consistent with the consecutive first-order kinetics for the hydrolysis of **1**. In a separate set of experiments, isolated **3**, when incubated in pH 7.4, 0.067 M sodium phosphate buffer at 38°C, degraded according to apparent first-order kinetics with a rate constant of 0.0500 ± 0.0018 min^{-1} (n = 3) or a $t_{1/2}$ of 13.9 min. The discrepancy of this value relative to that obtained for **3** during **1** hydrolysis is not understood but could be due to some difference in experimental conditions and/or methods of calculation.

Hydrolytic Products Identification—As shown in Table II, seven species in the **1** hydrolysate were identified as their trimethylsily derivatives by GC–MS under isobutane chemical ionization conditions. These are: **1**, **3**, **5**, **6**, **8**, **7**, and **9**. The identities of these seven components were based on the presence of quasi-molecular ions, relevant naturally occurring isotope peaks and their ratios to the parent or quasi-molecular ions, and other supportive mass fragments. All compounds as trimethylsilyl derivatives gave intense quasi-molecular ions. Compound **1** also gave an M + 3 fragment at approximately 60% of the intensity of the M + 1 peak, indicating the presence of two chlorine atoms. Compound **3**, in addition to the quasi-molecular ion at *m/z* 491 (base peak), gave a fragment at *m/z* 493, 49% of the height of the quasi-molecular ion (an increase from the expected 35% because of the contribution from silicon isotopes), indicating the presence of only one chlorine atom. Compound **5** gave an ion at *m/z* 545 as a base peak, and the absence of M + 3 indicates the loss of two chlorine atoms from **1**. Other fragments indicate appropriate cleavages that are consistent with the proposed structures as shown in Table II. The assignment of the relevant mass peaks to the appropriate quasi-molecular ion or fragments was further supported by the use of [β-$^2H_4$]**1** to generate these hydrolytic intermediates and products. GC–MS analysis gave corresponding increases in mass units for all of the relevantly labeled fragments (Table II). Moreover, when the slower-running peak in the HPLC eluant was isolated and subjected to GC–MS analysis, its mass spectrum was found to be identical to that in the hydrolytic mixture assigned to **3**, whereas the faster-running component was identical to the component assigned for **5**. Thus, their elution behaviors are consistent with the structures. The time sequence for their detection, i.e., **3** first followed by **5**, is also consistent with the hydrolysis mechanism (Scheme I, pathway a). The locations of phosphoramidic acid and phosphoric acid in the HPLC chromatogram were not known but were presumably eluted with the solvent front on the bases of their high polarity. Nor-nitrogen mustard and monohydroxy nor-

nitrogen mustard could not be located in the HPLC chromatogram due to a lack of chromophore at 207 nm. The structures of 1, nor-nitrogen mustard, and phosphoramidic acid detected in the hydrolytic mixture were further provided by the comparison of their mass spectra with those of the authentic samples. By using ^{31}P NMR, the solution of 1 gave five detectable signals other than that of 1 at the end of 2 h, indicating that at least a total of six phosphorus-containing species were present in the hydrolysis mixture (Fig. 7).

Structure of the Hydrolysis Intermediate—Engle et al.[14] reported the tentative identification of the aziridinium ion as a detectable intermediate in the degradation of 1 on the basis of ^{31}P NMR. The time course presented for this intermediate is essentially the same as that found for the species which we detected by both HPLC and ^{31}P NMR, wherein the HPLC visible species was subsequently identified as 3 by GC–MS. It was considered possible that this intermediate, initially detected both by ^{31}P NMR and by HPLC in our study, was indeed the aziridinium ion which, during the isolation and subsequent identification procedure, was converted to 3. However, the $t_{1/2}$ of 1 and the time course of this intermediate were essentially identical, as determined by ^{31}P NMR and HPLC under the same experimental conditions. Additionally, the eluate corresponding to this species was collected over a dry ice–acetone bath. Reinjection of the isolated intermediate onto the HPLC gave the same retention time as that of the originally detected species. Isolation of this component by HPLC gave a recovery of more than 75%, indicating that this component remained essentially intact during the manipulation. Thus, the results of these experiments strongly suggest that the intermediate detected by ^{31}P NMR is the same as that detected by HPLC and that this component is identical to the isolated species identified as 3 by GC–MS. Since incubation of [β-$^2H_4$]1 with high chloride concentration has led to the regeneration of 1 via the aziridinium ion, as evidenced by the scrambling of the labels, we reconstituted this isolated species in an aqueous solution containing 2 M NaCl to examine accumulation of 1 with time. The lack of 1 formation in this experiment indicated that there was no reversal to 1. On the basis of these results, the aziridinium intermediate reported by Engle et al.[14] was probably 3. Several investigations of degradation of compounds containing nitrogen mustard side chain have been reported.[19,28,29] None have reported the detection of the aziridinium ion intermediates. Our present results are consistent with these findings.

Effect and Mechanism of Chloride Ion Stabilization on Phosphoramide Mustard Solution—According to the degradation scheme (Scheme I), the stability of 1 is expected to be influenced by chloride ion concentration, as we have indeed observed (Fig. 10). As shown, the increase in $t_{1/2}$ appears to be linear with the increase of chloride ion concentrations, yielding a linear equation of: $t_{1/2} = 21.1[Cl^-] + 19.0$ by regression analysis, which is similar to the previously published equation[19] of: $t_{1/2} = 0.693k_{-1}[Cl^-]/k_1k_2 + 0.693/k_1$ where k_{-1}, k_1, and k_2 are the appropriate kinetic rate constants in that study. These results are in contrast with those obtained by Engle et al.,[14] who examined the degradation of 1 at different pH values in Tris or bis–Tris buffers. At pH values between 7.0 and 9.0, the half-lives for 1 degradation were similar to those obtained in our studies. However, at pH values lower than 7.0, the reported half-lives were at least threefold longer than that at the neutral pH and our values at comparable acidic conditions. The prolongation of half-lives of 1 was attributed solely to the pH effects in that study. It was noted that concentrated HCl was used to adjust the Tris or bis–Tris free base solutions to the desired pH values in that study. Therefore, the prolongation of the half-lives of 1 was probably due to the chloride ion stabilization effect. In the same study,[14] when 1 hydrolyses were carried out in the presence of various metallic chloride salts, Engle et al.[14] also observed prolongation of 1 $t_{1/2}$s. For example, the change from 1 M LiCl to 1 M $MgCl_2$ in pH 7.4 Tris buffer led to nearly a 50% increase in the $t_{1/2}$, and this result was attributed to the effect of the metallic ion. Although metallic ion might have certain effect on the stability of 1, the observed prolongation in the $t_{1/2}$ is also consistent with the extent of the chloride ion stabilization effect which we have measured here. Additionally, the hydrolysis of isolated 3, which possesses a single nitrogen mustard side chain, has also been found to be stabilized to fourfold in the presence of 2.0 M NaCl in our study. Other studies involving several nitrogen mustards also found that chloride ion causes an increase in the half-life of the parent compound in an aqueous solution.[19,30]

According to Scheme I, the first step for the formation of the aziridinium ion is generally considered to be reversible, and such a contention is reasonable on chemical grounds. However, actual experimental demonstration of the reversal is lacking. In addition, it is not understood whether the reverse reaction could occur appreciably, in both rate and extent, by overcoming the apparently thermodynamically favorable forward reaction with the chloride ion generated from the reaction (internal return). Moreover, the reversibility of this reaction by external chloride ion addition might have been the mechanism by which the previously observed stability in the presence of chloride ion was operating.[18,30] To this end, the question can be answered if 1, labeled with deuterium in the β position, is incubated in solutions containing chloride ion. Since the formation of aziridinium ion renders the two ethylene carbons symmetrical, the reverse reaction should result in scrambling of the labels (Scheme IIA). This scrambling can be monitored only if suitable mass fragmentation such as α-cleavage (M – CH_2Cl) is observed in mass spectrometry with proper derivatization of 1. This α-cleavage was not observed when silylation was used, but was detected in the trimethyl derivative of 1 under electron impact conditions. Thus, α-cleavage of the trimethyl derivative of 1 under electron impact conditions gave mass fragments at *m/z* 213 and 215, the latter of which is due to the chlorine isotope. With deuterium labels at the β positions, the corresponding fragments occurred at *m/z* 215 and 217. When scrambling occurred, the equivalent fragments would increase to masses at *m/z* 217 and 219, respectively (Scheme IIB). In this situation, however, mass at *m/z* 217 cannot be distinguished from the chloride isotope peak derived from mass at *m/z* 215 (α-cleavage fragment of unscrambled trimethyl [β-$^2H_4$]1. However, the fragment at *m/z* 219, representing the chloride isotope peak derived from the scrambled [β-$^2H_4$]1, appeared to be an appropriate ion to be monitored and reflects the scrambling. Thus, the ratio of 219/215 was used as an indicator, and the increase in this ratio with time is indicative of scrambling and reversal of the aziridinium ion formation.

Figure 11 shows that with no chloride ion addition, the ratio was very low and remained constant up to 100 min. Thus, this result indicated no appreciable reversal of the cyclization reaction within the time period of the experiment. This finding is also consistent with the contention of Engle et al.[14] However, with sodium chloride addition, such as 0.5, 1.0, and 2.0 M, the ratio increased with time, and the rate of increase was essentially parallel to the increase in chloride ion concentration. Therefore, these results provided evidence for both the formation of the aziridinium ion of 1 and the mechanism of the chloride ion stabilization effect. Similar mechanisms have been proposed to occur with chlorambucil[19] and is probably responsible for the stabilization effect of melphalan by chloride ion.[30] Further evidence for the presence of the aziridinium ion was obtained by incubating 1 in

1.0 M KBr and chromatographing the reaction mixture in the HPLC system. Under these conditions, a chlorine atom in **1** is expected to be replaced by a bromine through the aziridinium ion, forming the monobromo analogue of **1**. As the peak of **1** disappeared with time, a new peak emerged with a retention time longer than that of **1**. The height of this new peak continued to rise, reaching a plateau at about 12 min and thereafter decreasing in a first-order manner. When this component was isolated and analyzed by GC–MS as the trimethylsilyl derivatives, ions at *m/z* 481 and 483 at a ratio of approximately 1:1 were observed, indicating that the monobromo analogue of **1** had indeed formed.

Stability of Phosphoramide Mustard in Plasma and Human Serum Albumin—Compound **1** was found to degrade in fresh human plasma and in 5% human serum albumin solution in an apparent first-order manner with essentially identical degradation half-lives of 64 and 69 min (Fig. 12). Compared with the degradation of **1** in 0.067 M, pH 7.4 sodium phosphate buffer at 38°C ($t_{1/2}$ of 16 min), stability of **1** in either human plasma or human serum albumin was increased fourfold. This finding differs from that of Engle et al., who found no significant influence of bovine serum albumin on the stability of **1** in Tris buffer solution on the basis of ^{31}P NMR measurement.[14] This discrepancy may be due to difference in methodology or the protein and/or medium employed. The mechanism of stabilization of plasma and albumin on **1** in our study was not understood at present. However, this stabilization may modulate the pharmacokinetic behavior of **1** in vivo.

Compound **1** has been used clinically as an antitumor agent, but insufficient and pharmacokinetic information was available in time to guide its proper use relative to the formulation, dosage design, regimens, and scheduling. Compound **1** has since been found to be a major metabolite of cyclophosphamide and has been considered as the ultimate alkylating metabolite responsible for the antitumor activity of cyclophosphamide. The present stability study provides important information for consideration for preclinical or clinical evaluations of **1** as an antitumor agent. In addition, **1** undergoes rather complex hydrolysis to form a number of species, and some of these components may possess significant antitumor or other relevant pharmacologic activities. Recent studies from our laboratory have indicated that **1** or some of the hydrolytic products may have interesting immunomodulating activities.[31]

References and Notes

1. Friedman, O. M.; Seligman, A. M. *J. Am. Chem. Soc.* **1954**, *76*, 655–658.
2. Moddock, S. L.; Handles, H. A.; Friedman, O. M.; Foley, G. E.; Farber, S. *Cancer Chemother. Rep.* **1966**, *50*, 629–639.
3. Friedman, O. M.; Grublicuska, V.; Wodinsky, I. *Proc. Am. Assoc. Cancer Res.* **1963**, *4*, 21.
4. Nathanson, L.; Hall, T. C.; Putenberg, A.; Shadduck, R. K. *Cancer Chemother. Rep.* **1967**, *51*, 35–39.
5. Hall, T. C. *Cancer Chemother. Rep.* **1967**, *51*, 335–342.
6. Voelcker, G.; Wagner, T.; Hohorst, H. J. *Cancer Treat. Rep.* **1976**, *60*, 415–422.
7. Struck, R. F. *Cancer Res.* **1974**, *34*, 2933–2935.
8. Voelcker, G.; Draeger, U.; Peter, G.; Hohorst, H. J. *Arzneim. Forsch.* **1974**, *24*, 1172–1176.
9. Valente, E. J.; Chan, K. K.; Servis, K. L. *Pharm. Res.* **1984**, *2*, 89–92.
10. Colvin, M.; Brundrett, R. B.; Kan, M. N.; Jardine, I.; Fenselau, C. *Cancer Res.* **1976**, *36*, 1121–1126.
11. Fenselau, C.; Kan, M.-N.; Rao, S.; Myles, A.; Friedman, O. M.; Colvin, M. *Cancer Res.* **1977**, *37*, 2583–2543.
12. Engle, T. W.; Zon, G.; Egan, W. J. *Med. Chem.* **1979**, *22*, 897–899.
13. Zon, G. "NMR Studies of Drug Metabolism and Mechanism of Action"; in "Magnetic Resonance in Biology"; Cohen, J. S., Ed.; Wiley Interscience: New York, 1980; pp 116–118.
14. Engle, T. W.; Zon, G.; Egan, W. J. *Med. Chem.* **1982**, *25*, 1347–1357.
15. Since the concentrations of the species under study in all of the kinetic experiments were at least eightfold lower than the phosphate ion concentration, the pH was not changed appreciably at the end of the experiment. Thus, the definition "buffer" is not strictly followed.
16. Bryant, B. M.; Jarman, M.; Baker, M. H.; Smith, I. E.; Smyth, J. F. *Cancer Res.* **1980**, *40*, 4734–4738.
17. Gibaldi, M.; Perrier, D. "Pharmacokinetics"; Marcel Dekker: New York, 1975; pp 6–11.
18. Moon, R. B.; Richards, J. M. *J. Biol. Chem.* **1973**, *248*, 7276–7278.
19. Chatterji, D. S.; Yeager, R. L.; Gallelli, J. F. *J. Pharm. Sci.* **1982**, *71*, 50–54.
20. Bartlett, P. D.; Ross, S. D.; Swain, C. G. *J. Am. Chem. Soc.* **1947**, *69*, 2971–2977.
21. Bartlett, P. D.; Davis, J. W.; Ross, S. D.; Swain, C. G. *J. Am. Chem. Soc.* **1947**, *69*, 2977–2982.
22. Knevel, A. M.; Kehr, P. F. *Anal. Chem.* **1961**, *44*, 1863–1865.
23. Friedman, O. M.; Boger, E. *Anal. Chem.* **1961**, *33*, 906–910.
24. Golumbic, C.; Fruton, J. S.; Bergmann, M. J. *Org. Chem.* **1946**, *11*, 518–591.
25. Young, J. M.; Hiley, R.; Burgen, A. S. V. *J. Pharm. Pharmacol.* **1972**, *24*, 950–954.
26. Chan, K. K. *Drug Metab. Dispos.* **1982**, *10*, 474–479.
27. Chan, K. K.; Bolger, M. B.; Pang, K. S. *Anal. Chem.*, in press.
28. Chang, S. Y.; Alberts, D. S.; Farquhar, D.; Melnick, L. R.; Walson, P. D.; Salmon, S. E. *J. Pharm. Sci.* **1978**, *67*, 682–684.
29. Flora, K. P.; Cradock, J. C.; Kelley, J. A. *J. Pharm. Sci.* **1982**, *71*, 1206–1211.
30. Chang, S. Y.; Evans, T. L.; Alberts, D. S. *J. Pharm. Sci.* **1979**, *31*, 853–854.
31. Hengst, J. D.; Chan, K. K.; Mitchell, M. S. *Cell. Immunol.* **1985**, *90*, 218–294.

Acknowledgments

This work was supported in part by USC Cancer Center Core grant CA 14089-07 of the Pharmacoanalytic Unit and by grant CA 31693-01, both (KKC) from the National Cancer Institute and USPHS grant GM-08117 (PD) from the National Institute of General Medical Sciences. The use of the Southern California Regional NMR Facility at the California Institute of Technology was supported by NSF grant CHE 79–1632.

This study was presented in part at the 74th Annual Meeting of the American Association of Cancer Research, San Diego, CA, May 25–28, 1983 and as partial fulfillment for the Ph.D. requirement for E. Watson, School of Pharmacy, University of Southern California, Los Angeles, CA, 1985.